Hindawi Publishing Corporation
International Journal of Antennas and Propagation
Volume 2012, Article ID 639603, 7 pages
doi:10.1155/2012/639603

Review Article

A Large Aperture UWB Antenna Array for Real Beam Radar Imaging

Chao-Hsiang Liao and Dau-Chyrh Chang

Communication Research Center, Oriental Institute of Technology, No. 58, Sec. 2, Sichuan Road, Banqiao District, New Taipei 220, Taiwan

Correspondence should be addressed to Chao-Hsiang Liao, ot089@mail.oit.edu.tw

Received 17 October 2011; Revised 8 January 2012; Accepted 9 January 2012

Academic Editor: Deb Chatterjee

The development of four-element ultra-wideband (UWB) comb taper slot antenna array with 18 cm element spacing for real beam radar imaging is described. The four-element UWB array system with optimum element spacing is analyzed by energy pattern. A wideband double ridge horn antenna is used as the transmitting antenna, the developed large aperture UWB array is used as the receiving antenna. The transmitting antenna and the receiving antenna are combined with impulse time domain measurement system to achieve real beam radar imaging. The receiving impulse signals at various positions are processed by the time delay and sum algorithm. The examples of several aluminum cans have been verified in the resolution and compared with using the UWB array as a receive antenna and the double ridge horn as a transmit antenna in the test setup. The crossrange resolution of UWB antenna array is better than wideband double ridge horn antenna because the beam width of UWB array is narrower.

1. Introduction

In recent years, ultra-wideband (UWB) radars have become more and more attractive for microwave sensing and imaging applications [1, 2]. The short pulse duration of only a few picoseconds offers the advantage of a high range resolution leading to ground penetrating radar (GPR) applications through wall imaging or contactless material testing [3–5]. The UWB array waveform is an effective way of improving the resolution for microwave imaging. The pulse width is an important factor that affects the angular resolution of UWB antenna array. Angular resolution can be enhanced by increasing the number of array elements, the interelement spacing, or signal bandwidth. They can be modeled to use short pulse techniques to implement high range resolution while directing energy in a particular direction. Consequently, accurate position determination and tracking of objects are possible with UWB signals. This makes an UWB array with impulse waveforms suitable for radar direction finding and imaging applications. These applications require the understanding of the characteristics and specialties of UWB antenna arrays.

The application of UWB arrays leads to narrow beam widths for sparse arrays with large element spacing. To provide high-resolution radar imaging, the antenna beam width should be narrow. Since the 3 dB beamwidth of the antenna array is inversely proportional to the size of the aperture, the larger aperture of the UWB array produces a narrower beamwidth. Unfortunately, a larger aperture UWB array with larger element spacing generates periodic grating lobes in the power pattern; it is impossible to have large array aperture size with small quantity of antenna elements. However, the grating lobes do not occur in the energy pattern, even if the element spacing of the array is larger than one wavelength [6]. If using the energy pattern's concept, it is easier to get high-resolution radar imaging by a larger aperture of an UWB array with larger element spacing. In this study, this concept will be used in proposed real beam radar imaging. A large aperture UWB array by sparse antenna element can be constructed to achieve high angular resolution without encountering the problem of grating lobes.

UWB excitation and synthetic aperture radar (SAR) technologies can be employed in order to obtain good image

resolution. There are different radar measurement techniques to present image, including monostatic, bistatic, and multistatic. For creating synthetic focal point, some beamforming methods have been provided, such as time delay and sum scheme [7, 8], microwave imaging via space-time beamforming (MIST) method [9–12], robust weighted Capon beamforming (RWCB) method, and multistatic adaptive microwave imaging (MAMI) method [13, 14]. Different data process methods provide different resolutions and interference rejection capability.

For UWB array radar system, the received data is often processed using conventional "time delay-and-sum beamforming." In this method, the output is formed by summing weighted and delayed versions of the received signals. The delays used for each antenna position are determined by the array geometry and the desired look direction, while this approach is straightforward and easy to implement. This UWB radar architecture has many desirable features, including a wide bandwidth, short-duration range gating, high dynamic range, high sensitivity, and low transmitted power. Base on the principles of UWB SAR techniques, an UWB real beam radar imaging system will be developed. In this paper, it will be shown that a low-power and high-sensitivity UWB array is suitable for real beam radar imaging system, based on commercially available pulse generator, digital sampling converter, time delay-and-sum beamforming algorithm.

This paper is organized as follows. Design considerations for a large aperture UWB antenna array are presented in Section 2: UWB Antenna Array with Optimum Element Spacing. The development of the UWB real beam radar imaging system is described in Section 3: UWB Real Beam Radar Imaging System. The imaging reconstruction algorithm is presented in Section 4: Imaging Reconstruction Algorithm, and the measurement results are presented in Section 5: Measurement Results. Main 4 conclusions of this study are summarized in Section 6: Conclusion.

2. UWB Antenna Array with Optimum Element Spacing

Large two-dimensional arrays are essential for high-resolution two-dimensional imaging but must be highly thinned to avoid an unrealistic cost, difficult electronic fabrication problems, and handling of an enormous data flow for real-time computation. Microwave imaging often requires side lobe control or via weighting of the frequency domain aperture. Side lobe improvement using spectral weighting is invariably at the expense of main lobe resolution [15, 16]. These images are plagued with artifacts caused by high side lobes. Specifically, these artifacts are false targets and target breakup or speckle.

In this section, the four-element UWB array system with large uniform and nonuniform element spacings is analyzed by energy pattern. The performance analysis of side lobe level of UWB antenna array for real beam radar imaging is shown. The UWB antenna array is composed of four UWB comb tapered slot antenna elements aligned in the H-plane, a multistage, with a four-way microstrip UWB power divider,

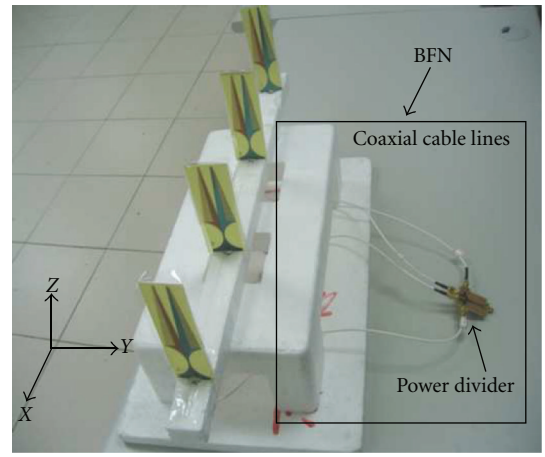

Figure 1: H-plane UWB antenna array.

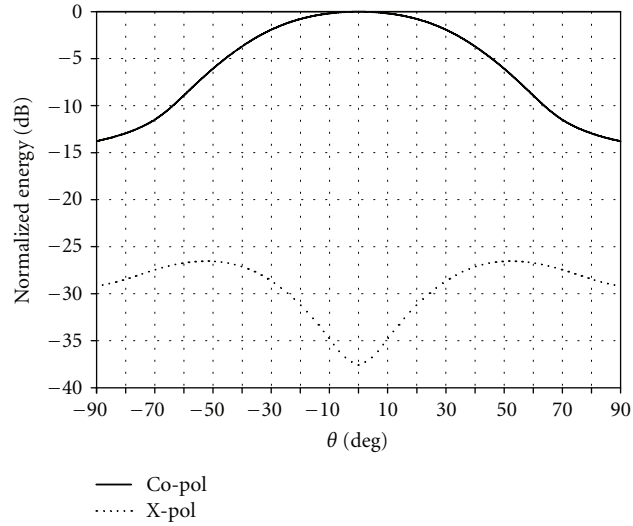

Figure 2: H-plane energy pattern of comb taper slot antenna by simulation (X-Z plane).

and four identical coaxial cable lines (ULA-316), as shown in Figure 1. Figure 2 shows the H-plane energy patterns of the comb slot antenna element by simulation. The energy pattern of the antenna is the total response of the power patterns in the frequency domain. This provides a simple representation of antenna behavior as that of a large number of power patterns. It is easier to describe the energy pattern, instead of the power pattern, for UWB antennas and arrays [6].

There are five types of UWB antenna arrays with different middle element spacing in array aperture of 54 cm, they are described and compared here. Type one (linear array) is UWB array with element spacing of 18 cm. Type two (Case A) is UWB array with middle element spacing of 8 cm. Type three (Case B) is UWB array with middle element spacing of 5 cm. Type four (Case C) is UWB array with middle element spacing of 28 cm. The type five (Case D) is UWB array with middle element spacing of 38 cm. Figures 3 and 4 show the simulation results of the H-plane energy pattern for

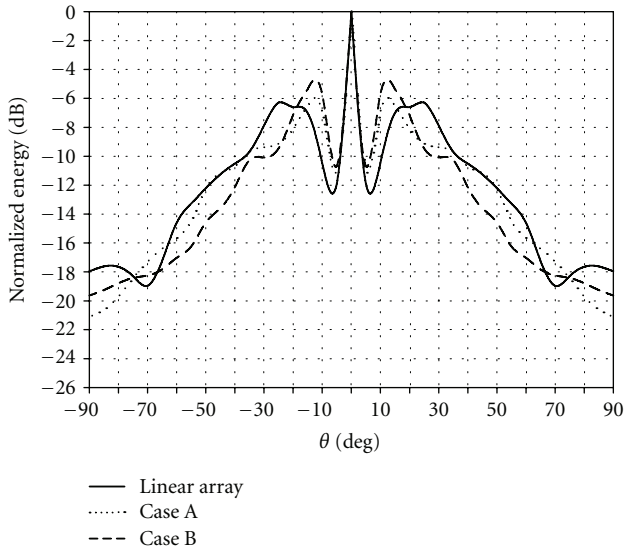

Figure 3: Comparison of energy pattern for four-element array with reduced middle element spacing (X-Z plane).

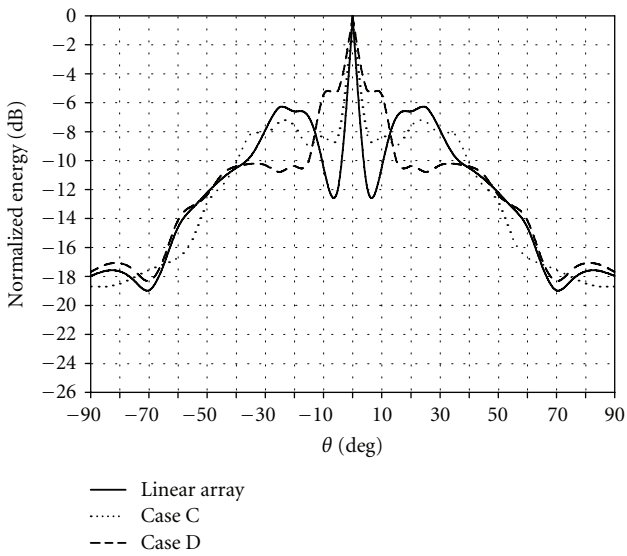

Figure 4: Comparison of energy pattern for four-element array with incremental middle element spacing (X-Z plane).

four-element arrays with reduction and increment middle element spacing. From the above results, if the array is with reduced middle element spacing, the peak side lobe level of the energy pattern will be higher and close to the mainbeam; if the array is with incremental middle element spacing, the peak side lobe level of the energy pattern will be lower and the first null side lobe level will be higher. This is caused by the antenna element energy pattern. Because the energy pattern of UWB antenna array is the convolution of the antenna element transient response with the time-domain array factor.

Summary of above five types UWB arrays, type one (linear array) is suitable for real beam radar imaging due to the side lobe level and fist null side lobe level are lower, as

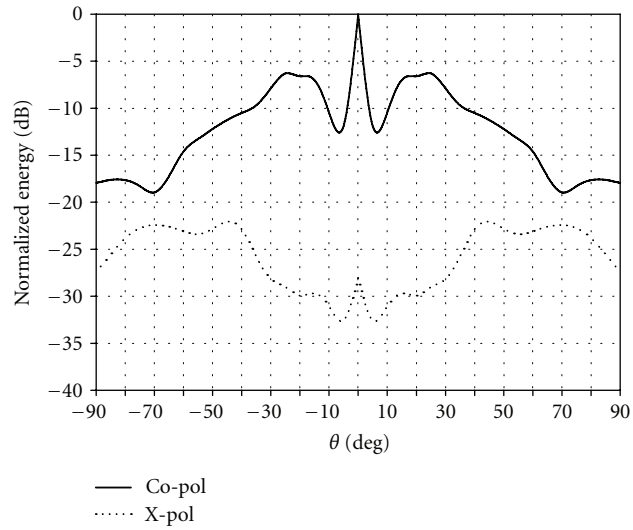

Figure 5: H-plane energy pattern of UWB linear array by simulation (X-Z plane).

shown in Figure 5. Since the element spacing of linear array is large than 1.5 wavelength at the lowest frequency, the mutual coupling is small. The impact of high side lobe level depends on the application of the array. For radar application, the false alarm target may be confused with high peak side lobe level. For the application of point-to-point communication, minor fading may be occured with high peak side lobe level. In general, the optimum design of array element spacing is required for special application.

3. UWB Real Beam Radar Imaging System

The impulse time response waveform and the narrow beamwidth of an UWB array are good for high-resolution radar imaging. Several types of antennas have been utilized in UWB array applications, including horn, Vivaldi, and patch antennas [17]. The selection of antenna will eventually depend on a system's requirement on portability and bandwidth. The pulse generator and antenna would require custom implementation for their critical requirement on UWB performance.

The proposed system consists of a single transmitting wideband double ridge horn antenna, the four-element UWB comb taper slot antenna array with 18 cm element spacing as the receiving antenna, and impulse time domain radar system. The hardware implementation of the proposed UWB array real beam radar system and a 200 cm of linear scanner are shown in Figure 6. The target is placed on the linear scanner, and the antennas are mounted on wood shelves to acquire target profile. The impulse Gaussian signal with the pulse repetition frequency of 250 KHz is used during the measurement, that is, the pulse period is 4 μs. The impulse generator is a Gaussian pulse with pulse width 30 ps and amplitude 20 V. The receiver is a wideband digital sampling oscilloscope. The receiver has an instantaneous bandwidth of 26 GHz and a linear dynamic range of 66 dB. The output impedance for the trigger generator and digital

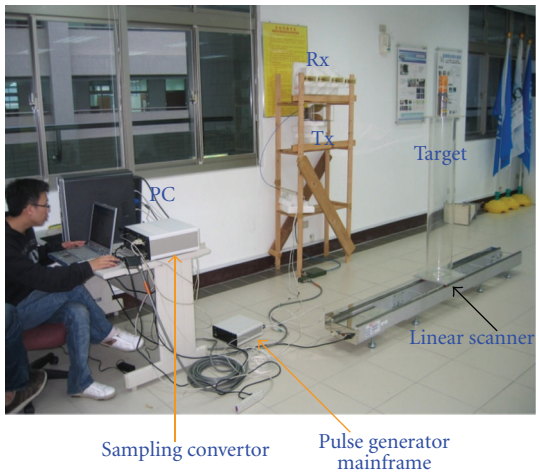

Figure 6: UWB array quasimonostatic real beam radar imaging system.

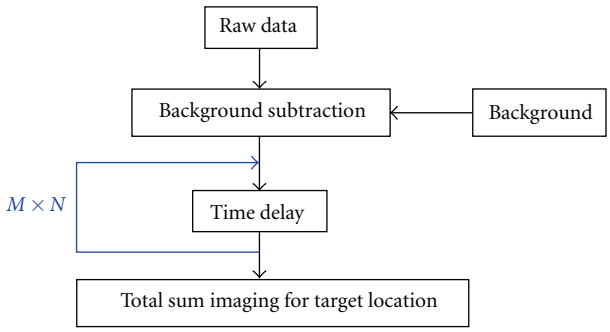

Figure 7: Imaging reconstruction flowchart.

sampling oscilloscope are 50 ohm. The observation time window can be varied from 10 ps to 2000 ns with variable acquisition data points from 4 to 4096.

The transmitting antenna and the receiving antenna are placed close to each other for quasi monostatic architecture. The total scan length is 200 cm with 200 sample points. The impulse Gaussian signal is transmitted through the wideband double ridge horn antenna. The target reflects impulse Gaussian signal toward the UWB array to register backscattered waveform. Time delays are applied to receive impulse signals at various positions to generate the down range data. The sum of each time delay to achieve an image.

4. Imaging Reconstruction Algorithm

Spatial focusing of the backscattered waveforms can be achieved with a simple time delay and sum beamforming approach, the backscattered waveform recorded at the antenna locations include early and late time content. There are $U + 1$ quasi monostatic impulse sample signals when radar is linear scanned along x direction with total length S_{U+1}. x-axis is cross range direction and y-axis is down

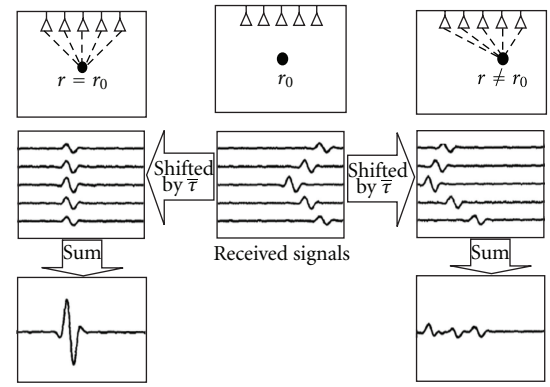

Figure 8: Diagram of time delay and sum method.

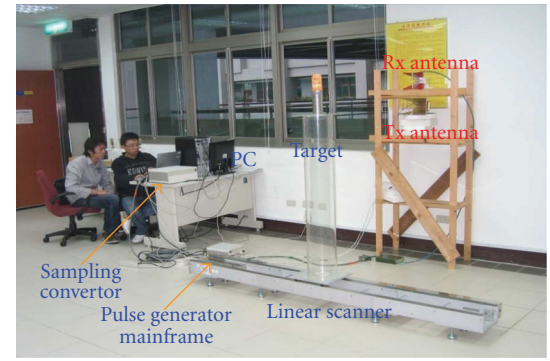

Figure 9: Wideband double ridge horn quasi monostatic real beam radar imaging system for example 1.

range direction. The magnitude of scattering signal P at pixel (x_m, y_n) can be expressed as

$$P(x_m, y_n) = \sum_{u=1}^{U+1} S_u(t-\tau), \tag{1}$$

where

$$\tau = \frac{2\left(\sqrt{(x_u - x_m)^2 + (y_u - y_n)^2}\right)}{C}, \quad x_u = u\Delta x, \quad x_m = m\Delta x, \quad y_n = n\Delta y. \tag{2}$$

$S_u(t)$ is the received time domain sample data, (x_u, y_u) is the radar position, τ is the round trip time delay between pixel (x_m, y_n) and radar position (x_u, y_u), (x_m, y_n) is the image position, D_x, D_y is the imaging area, $\Delta x = D_x/M$ is the resolution in cross range, $\Delta y = D_y/N$ is the resolution in down range, Δt is the pulse width, and C is the light velocity.

The detail imaging processing flowchart is shown in Figure 7. First, the receiving impulse signals at various positions are acquired as raw data. Second, the target position and the background are subtraction. The radar system needs to take data twice, one is background with target, and another one is only background, and then background can be subtracted to get the target information. Third, the time

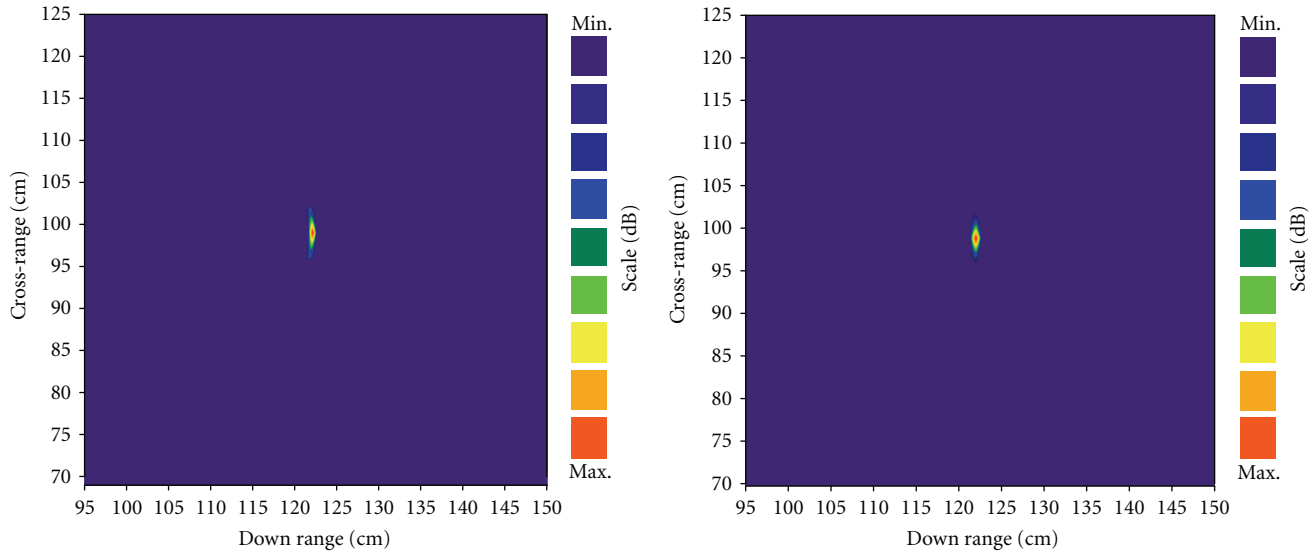

Figure 10: UWB radar imaging for example 1 by measurement. (a) Wideband double ridge horn antenna and (b) UWB array quasi monostatic architecture.

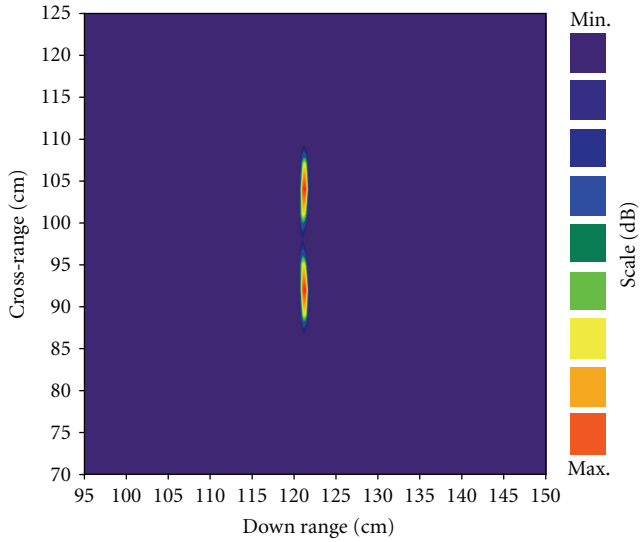

Figure 11: Microwave imaging for example 2.

delay and total sum imaging for target location is shown in Figure 8, the received signals are shown in the central panel, when the beamformer is steered to lo-cation r_0 (the actual location of a scatter), the signals coher-ently sum, as shown by the left panel; when the beamformer is steered to a location other than r_0, incoherent summation results, as shown by the right panel.

5. Measurement Results

There are four examples of aluminum cans that will be verified in the proposed UWB real beam radar imaging system. In order to prove that the UWB array can improve the imaging resolution, in this section also compared with transmitting and receiving antennas are wideband double ridge horn antenna, as shown in Figure 9. Example one is an aluminum can. x-axis is cross-range direction and Y axis is down range direction. The diameter of aluminum can is about 5 cm and placed on (X: 98 cm, Y: 122 cm), as shown in Figure 10, the imaging results are including wideband double ridge horn antenna and UWB array quasi monostatic architectures, the cross-range resolution of UWB antenna array is better than single wideband double ridge horn antenna because the beam width of UWB array is narrower.

Example two is two identical aluminum cans and separation 5 cm by UWB array measurement. The diameter of aluminum can is about 7 cm, placed on (X: 92 cm, Y: 122 cm) and (X: 104 cm, Y: 122 cm), as shown in Figure 11.

Example three is two identical aluminum cans, placed on different position by UWB array measurement. The diameter of aluminum can is about 7 cm, placed on (X: 92 cm, Y: 122 cm) and (X: 105 cm, Y: 135 cm), as shown in Figure 12.

Example four is two different aluminum cans, placed on different position by UWB array measurement. The diameter of small aluminum can is about 4 cm and it is placed on (X: 115 cm, Y: 95 cm), the diameter of large aluminum can is about 6 cm and it is placed on (X: 87 cm, Y: 123 cm) as shown in Figure 13. The target locations and imaging results of four examples are almost the same.

6. Conclusion

The four-element UWB array systems with uniform and nonuniform element spacings are analyzed by energy pattern. There are five types of UWB antenna arrays with different middle element spacing in array aperture of 54 cm

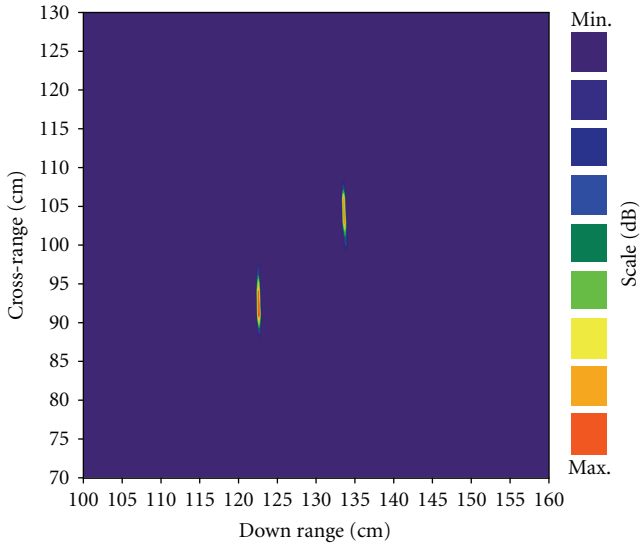

Figure 12: Microwave imaging for example 3.

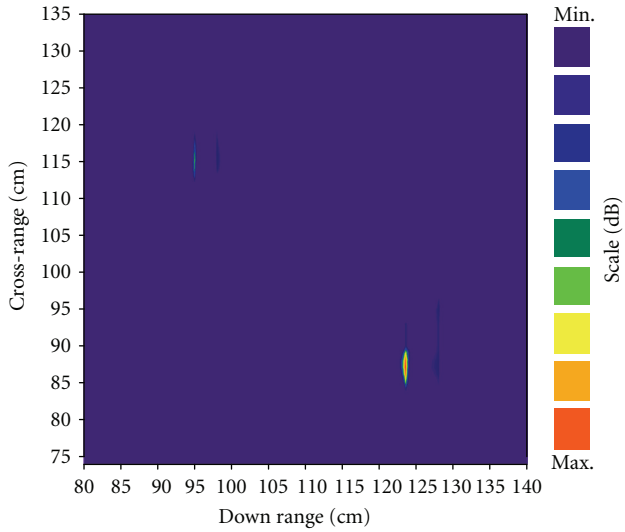

Figure 13: Microwave imaging for example 4.

that are discussed. Linear UWB antenna array is suitable for real beam radar imaging because the side lobe level and fist null side lobe level are lower.

UWB array quasi monostatic radar architecture is presented for real beam radar imaging. The transmitting antenna is a wideband double ridge horn antenna. The receiving high directivity antenna is a four-element UWB antenna array with total aperture size of 54 cm. By using the time delay and sum algorithm, the magnitude and location of the target can be built. The examples of several aluminum cans are verified in the proposed UWB real beam radar imaging system. The results of real beam radar imaging from measurement structure are in agreement. This radar architecture could be used for RCS measurement, or other radar applications.

The first experimental results have shown that the system successfully detected small metal targets. In the next stage of the research program, dedicated software for real-time image processing, localization, and classification of targets will be embedded into the real beam radar system. The developed approach can be used in other applications such as medical imaging, area surveillance, road and runway inspection, and others.

References

[1] A. M. Zoubir, I. J. Chant, C. L. Brown, B. Barkat, and C. Abeynayake, "Signal processing techniques for landmine detection using impulse ground penetrating radar," *IEEE Sensors Journal*, vol. 2, no. 1, pp. 41–51, 2002.

[2] A. Benedetto, F. Benedetto, M. R. De Blasiis, and G. Giunta, "Reliability of signal processing technique for pavement damages detection and classification using ground penetrating radar," *IEEE Sensors Journal*, vol. 5, no. 3, pp. 471–479, 2005.

[3] S. Vitebskiy, L. Carin, M. A. Ressler, and F. H. Le, "Ultra-wideband, short-pulse ground-penetrating radar: simulation and measurement," *IEEE Transactions on Geoscience and Remote Sensing*, vol. 35, no. 3, pp. 762–772, 1997.

[4] J. S. Lee, C. Nguyen, and T. Scullion, "A novel, compact, low-cost, impulse ground-penetrating radar for nondestructive evaluation of pavements," *IEEE Transactions on Instrumentation and Measurement*, vol. 53, no. 6, pp. 1502–1509, 2004.

[5] Y. Yang and A. Fathy, "Design and implementation of a low-cost real-time ultra-wide band see-through-wall imaging radar system," in *Proceedings of the IEEE MTT-S International Microwave Symposium (IMS '07)*, pp. 1467–1470, June 2007.

[6] C.-H. Liao, P. Hsu, and D.-C. Chang, "Energy patterns of UWB antenna arrays with scan capability," *IEEE Transactions on Antennas and Propagation*, vol. 59, no. 4, pp. 1140–1147, 2011.

[7] S. C. Hagness, A. Taflove, and J. E. Bridges, "Two-dimensional FDTD analysis of a pulsed microwave confocal system for breast cancer detection: fixed-focus and antenna-array sensors," *IEEE Transactions on Biomedical Engineering*, vol. 45, no. 12, pp. 1470–1479, 1998.

[8] X. Li and S. C. Hagness, "A confocal microwave imaging algorithm for breast cancer detection," *IEEE Microwave and Wireless Components Letters*, vol. 11, no. 3, pp. 130–132, 2001.

[9] P. M. Meaney, M. W. Fanning, D. Li, S. P. Poplack, and K. D. Paulsen, "A clinical prototype for active microwave imaging of the breast," *IEEE Transactions on Microwave Theory and Techniques*, vol. 48, no. 1, pp. 1841–1853, 2000.

[10] E. C. Fear, S. C. Hagness, P. M. Meaney, M. Okoniewski, and M. A. Stuchly, "Enhancing breast tumor detection with near-field imaging," *IEEE Microwave Magazine*, vol. 3, no. 1, pp. 48–56, 2002.

[11] S. K. Davis, H. Tandradinata, S. C. Hagness, and B. D. Van Veen, "Ultrawideband microwave breast cancer detection: a detection-theoretic approach using the generalized likelihood ratio test," *IEEE Transactions on Biomedical Engineering*, vol. 52, no. 7, pp. 1237–1250, 2005.

[12] E. C. Fear, X. Yun, and R. H. Johnston, "Radar-based microwave Imaging for breast cancer detection: tumor sensing with cross-polarized reflections," in *Proceedings of the IEEE Antenna and Propagation Society International Symposium*, pp. 2432–2435, June 2004.

[13] P. Stoica, Z. Wang, and J. Li, "Robust Capon beamforming," *IEEE Signal Processing Letters*, vol. 10, no. 6, pp. 172–175, 2003.

[14] Y. Xie, B. Guo, J. Li, and P. Stoica, "Multistatic adaptive microwave imaging for early breast cancer detection," *IEEE*

Transactions on Biomedical Engineering, vol. 49, pp. 812–822, 2002.

[15] L. J. Porcello, "Speckle reduction in synthetic-aperture radars," *Journal of the Optical Society of America*, vol. 66, no. 11, 1975.

[16] B. D. Steinberg, *Microwave Imaging with Large Antenna Arrays*, Wiley, New York, NY, USA, 1983.

[17] Y. Yang, Y. Wang, and A. E. Fathy, "Design of compact Vivaldi antenna arrays for UWB see through wall applications," *Progress in Electromagnetics Research*, vol. 82, pp. 401–418, 2008.